Development and use of garnet-based high-resolution P-T-t paths to constrain the dynamics of Himalayan orogenesis

Elizabeth J. Catlos[1], Theresa Perez[1], Thomas Etzel[1], Oscar Lovera[2]
1: Jackson School of Geosciences, University of Texas at Austin, TX, USA
2: UCLA, Earth and Planetary Sciences, CA, USA

INTRODUCTION. The Main Himalayan Thrust (MHT) is a pervasive décollement that separates the down-going Indian plate from the Himalayan orogenic wedge (Fig. 1). The structure is responsible for a significant component of the present-day seismicity of the Himalayan range and is considered one the largest and fastest slipping continental megathrusts on Earth. Understanding the geometry and history of the development of the MHT and the large-scale fault systems that splay into the structure has implications for assessing and predicting the hazard impacts of major event Himalayan earthquakes, including their initiation, propagation, and termination. However, the MHT has an uncertain topography.

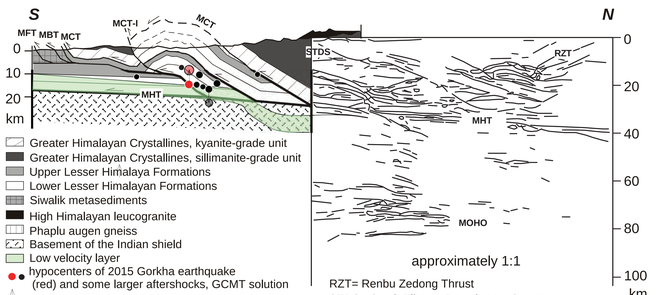

Figure 1. Balanced, deformed-state, cross-section through the eastern Himalaya at about longitude 87.3°E (Schelling and Arita, 1991) connected to a seismic reflection profile (Zhao et al., 1993). The section illustrates the juxtaposition of tectonostratigraphic units across the major Himalayan faults and interprets the Lesser Himalaya as a hinterland-dipping duplex. The low-velocity layer and hypocenter of the Mw7.8 Gorkha earthquake (red circle) and some larger aftershocks (black circles) are also plotted after Arora et al. (2017). We include the GCMT and USGS solutions of the Gorkha earthquake hypocenters and its aftershocks. The locations of the hypocenters for both datasets agree, except for two of the earthquakes selected by Arora et al. (2017).

The 2015 April 25th Mw 7.8 Gorkha earthquake in central Nepal called attention to the problem regarding the subsurface geometry of the MHT. Most attribute the main shock to reverse fault displacement along the MHT. Still, the Gorkha earthquake, or at least some of its aftershocks, may have nucleated above the MHT within the Lesser Himalaya Formation (LHF) duplex system. An aftershock of the Gorkha earthquake lies along the Main Central Thrust (MCT). The idea of a presently seismogenic MCT and the potential for activity within the duplex has been proposed several years before the Gorkha event based on focal plane solutions for earthquake events in western Nepal and India. Alternatively, the shallower events are explained by a segmented MHT that includes a ramp.

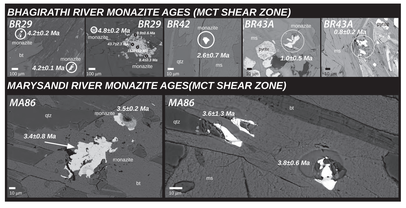

Figure 2. Young monazite ages from rocks collected from the Main Central Thrust shear zone. (Upper) Marsyandi River Transect (Catlos et al., 2001; 2018) and (lower) Bhagirathi River transect (Catlos et al., 2007). See Figure 3 for sample locations.

The ability exists now to generate high-resolution P-T paths from garnet-bearing rocks from within the LHF duplex system to understand how rocks within the MCT zone grew due to changes in their environmental conditions. However, the applicability of the garnet-based paths to deciphering the present-day dynamics and possible architecture of the LHF duplex system requires that the geometric constraints of Himalayan architecture remained constant over the last few million years. Because Pliocene-age and younger monazite (REEThPO4) grains exist within the MCT shear zone in central Nepal and NW India (1-4 Ma, Fig. 2), these locations may be helpful in lending insight into the present-day framework and dynamics of the Himalayas.

METHODS. We report high-resolution garnet P-T paths and new monazite ages from both the hanging wall and footwall of the MCT from along the Bhagirathi River in NW India and Marysandi River in central Nepal (Fig. 2). The Bhagirathi River region experienced an Mw 6.8 earthquake in 1991 (Uttarkashi earthquake, 21:23:14, 30.7800° 78.774°, USGS). Like the Gorkha earthquake, the reported hypocenter depth varies (10, 10.3, 12, 15, 16.1, 19.0 km; USGS catalog, GCMT focal depth, Yu et al., 1995; Cotton et al., 1995; Sandeep et al., 2014).

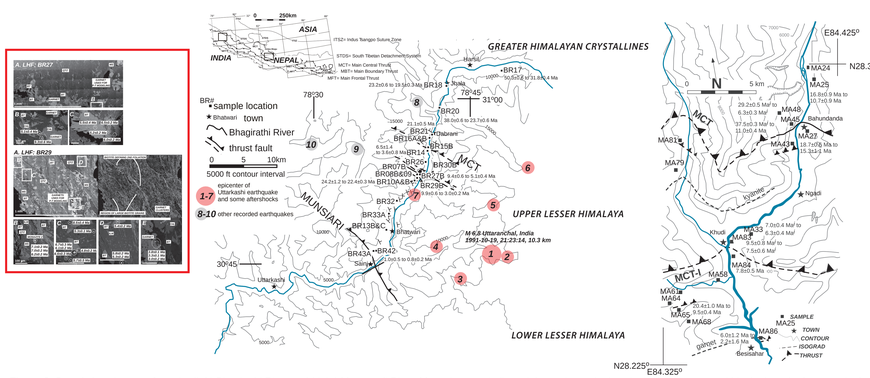

Figure 3. Sample location map from the (left) Bhagirathi River and (right) Marysandi River. Monazite ages indicated. Inset shows the locations of the transect within the broader framework of the Himalayan fault systems. The Bhagirathi River shows the epicenter of the Uttarkashi earthquake and its aftershocks (numbered 2-7; USGS catalog), as well as the epicenter of other earthquakes in the area. BSE images show new monazite ages from MCT footwall samples BR27 and BR29.

Rocks in this study were collected across the MCT shear zone (Catlos et al., 2001; 2007; 2018) (Fig. 3). All samples are Al-rich Himalayan pelitic schists and gneisses and contain garnet + biotite ± plagioclase ± aluminosilicate + muscovite + quartz with accessory minerals monazite, zircon, tourmaline, rutile, and/or ilmenite. The MCT shear zone itself has an upper and lower bound, with its lower structure in this region termed the Munsiari Thrust or MCT-I. Conventional P-T conditions and Th-Pb ion microprobe monazite ages exist from some of the assemblages modeled here (Table 1; Fig. 3). In some cases, conventional pressures were unable to be estimated due to the lack of minerals used in the calibration.

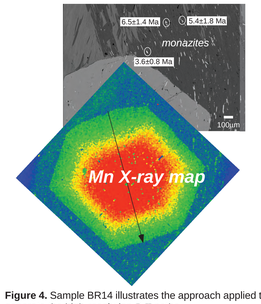

Figure 4. Sample BR14 illustrates the approach applied to generate the high-resolution P-T paths.

A. STEP 1. Create an isochemical phase diagram using rock bulk composition. Overlie garnet core composition isopleths.
B. STEP 2. Generate compositional transects across garnets in the rock-- Smooth compositions.
C. STEP 3. Use Matlab script to apply the Theriak-Domino program (de Capitani & Brown, 1987; de Capitani & Petrakakis, 2010; Moynihan and Pattison, 2013) to generate P-T paths.
D. STEP 4. Generate isochemical phase diagram for the garnet rim-- Overlie garnet rim and matrix mineral compositions.

STEP 5. Compare modeled P-T path with the smoothed and raw data. Compare with conventional P-T conditions.

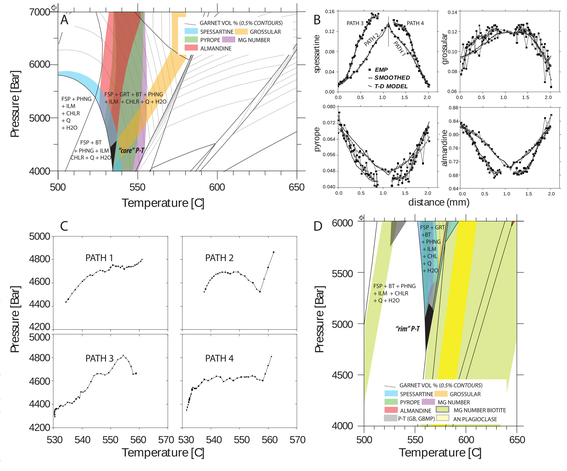

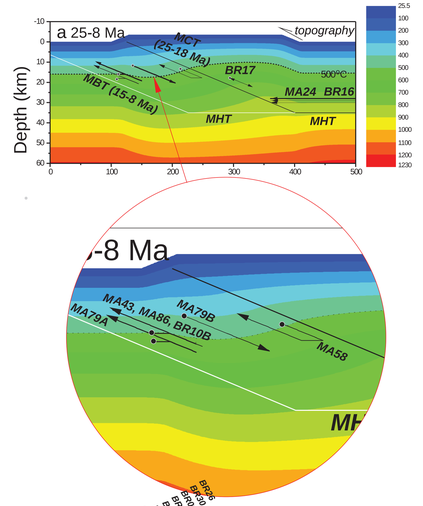

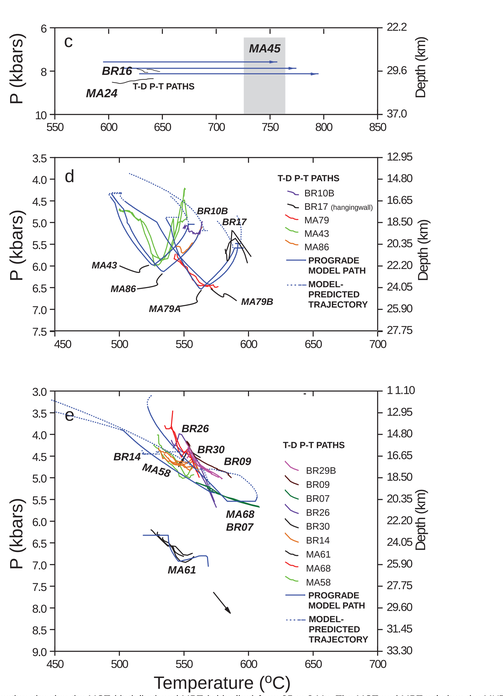

Figure 4. After Harrison et al. (1998) and Catlos et al. (2018). **(a)** Thermal-kinematic model cross-section showing the MCT (dark line) and MBT (white line) from 25 to 8 Ma. The MCT and MBT sole into the MHT at depth. Isothermal sections in degree increments are indicated by the color scale bar. Panel **(a)** is meant to show the thermal situation at 18 Ma after MCT slip. Rock trajectories are represented by arrows with dots at the initial and heads at the final position. Samples MA24 and BR16 are labeled, and three different possible tracks for this rock are shown. The inset shows the locations of samples MA58, MA43, MA86, and two options for the position of sample MA79. The MCT is active from 25 to 18 Ma, whereas slip transfers to the MBT from 15 to 8 Ma. **(b)** The model cross-section of the thermal evolution of the MCT shear zone from 8 to 2 Ma. In this case, the MCT and MCT-I sole into the MHT at depth. This panel represents the thermal situation at 6 Ma. Sample trajectories are shown for the MA and BR samples. **(c)** P-T paths for Greater Himalayan Crystallines sample MA24 and three options for possible matching trajectories. We also indicate P-T conditions for GHC sample MA45 (Table 1). **(d)** P-T paths generated using the Theriak-Domino model approach and those predicted by the thermal model. **(e)** P-T paths are plotted for samples in panel **(b)**. In both **(d)** and **(e)**, dashed lines show the retrograde portion of the paths (decreasing T) or continued movement through the model (increasing T).

Table 1. *Summary of P-T conditions of samples analyzed.*

Sample[a]	GB T (°C)[b]	GPBM P (kbar)[c]	T-D core P (kbar)[d]	T-D core T (°C)[d]	T-D rim P (kbar)[e]	T-D rim T (°C)[f]	QuiG P (kbar) [at T(°C)][g]
Greater Himalaya Crystallines							
MA24	600±18	9.32±0.37	580±50	8.65±1.20	640±7	8.60±28	
MA45	745±20	11.50±0.50					6.81±0.50 (550°C)
BR17			582±5	5.67±0.50	600±5	5.86±0.10	
BR21	730±25	>10	680±4	7.19±0.20	682±10	9.39±0.25	
BR16B			630±8	7.90±0.40	642±10	8.04±0.25	
Upper Lesser Himalaya Formation							
MA27	635±20	7.80±1.00					
MA43	650±20	8.78±0.74	490±3	4.75±0.25	553±4	4.58±0.25	6.87±0.80 (500°C)[j] 6.15±0.43 (560°C)
MA79	523±53		544±6	5.70±0.28	573±4	6.63±0.18	6.44±0.53 (550°C)
MA33	565±15	6.50±0.50					6.57±0.42 (540°C)
MA83	550±25						
BR14	540±25	7.00±1.8	534±5	4.40±0.40	561±10	4.80±0.50	
BR26	570±21		541±4	4.20±0.20	574±5	5.60±0.10	
BR30B			546±1	4.73±0.20	557±20	4.49±0.25	
Lower Lesser Himalaya Formation							
MA58	508±38		533±4	4.20±0.28	560±7	5.00±0.42	
MA61	550±25	8.26±0.58	523±4	6.18±0.18	557±5	6.75±0.21	7.92±56 (535°C)
MA64	475±35		525±1	4.25±0.21	555±2	4.38±0.25	
MA65	525±30	7.34±0.90	535±4	4.20±0.28	554±6	4.50±0.14	7.08±0.60 (550°C)
MA68	513±38		538±4	3.83±0.39	565±10	>5	
MA86	530±25	6.98±0.64	547±5	5.50±0.21	568±4	5.20±0.28	
BR07	595±25		559±5	5.10±0.10	608±50	>5.7	
BR27B			558±15	4.87±1.00	566±10	4.85±0.25	
BR09	630±50	8.20±0.70	553±5	4.25±0.20	586±25	5.02±1.00	
BR29B			552±4	4.31±0.50	575±20	4.95±0.50	
BR10B	720±50	9.1±2.00	549±4	5.12±0.40	564±10	4.97±0.40	

a. Samples from both transects are arranged in order from hanging wall to structurally lowest.
b. Temperatures determined using garnet-biotite (GB) thermometry (Ferry & Spear, 1978; Berman, 1990) with uncertainty representing the range of conditions at the specified pressures. If no P was measured, these temperatures represent the conditions from 0 to 10000 bars (from Catlos et al. 2001). Other thermometers could be applied and re-estimated, but we report these conditions as the thermal-kinematic model discussed relied on these conditions for development.
c. Pressures determined using garnet-plagioclase-biotite-muscovite (GPBM) barometry (Hoisch, 1990) (from Catlos et al. 2001). Other barometers could be applied and re-estimated, but we report these conditions as the thermal-kinematic model discussed relied on these conditions for development.
d. Temperature estimate for the core of the garnet using Theriak-Domino.
e. Pressure estimate for the core of the garnet using Theriak-Domino.
f. Temperature estimate for the rim of the garnet using Theriak-Domino.
g. Pressure estimate for the core of the garnet using Theriak-Domino.
h. Quartz inclusions in garnet P conditions at a specified T. Four inclusions were measured in sample MA61, three in sample MA33 and MA43 (core), two in samples MA65, MA79, and MA43 (rim), and one in sample MA45.
i. Blank space = not measured.
j. The first value is for three inclusions in the core, and second value is average of two values in the garnet rim.

RESULTS. High-resolution P-T paths were input into the thermokinematic model of Harrison et al. (1998), where thermobarometric histories are calculated using a two-dimensional finite-difference solution to the diffusion-advection equation. The model fits the P-T paths, if the MCT speed rate is 5 km/Ma between 25 and 18 Ma and a progressive topography builds to 3.5 km. A pause in slip is introduced for the MCT between 18 and 15 Ma, which represents the initiation and transfer of activity to the MBT. During this time, denudation of the buildup topography is active at a rate of 1.5 km/Ma.

The majority of the high-resolution P-T paths from both transects fit the modified Harrison et al. (1998) modeled P-T paths and thus implies that the MCT may have experienced a period of quiescence during the onset of the MBT. Activation of thrusts within the MCT footwall from 8 to 2 Ma suggests a high rate of exhumation (>12 mm/yr) since the Pliocene.

The Theriak-Domino P-T paths cannot be reproduced by the Harrison et al. (1998) model if only a single phase of Miocene MCT motion is imposed. The P-T paths themselves require footwall imbrication and the outlined modifications.

The results suggest that both MCT footwall imbrication and slip along the MHT should be considered in developing Himalayan architecture and assessing its seismic hazard.